Crystal Structures of HIV-1 Reverse Transcriptase in Complex with Carboxanilide Derivatives[†,‡]

Jingshan Ren,[§] Robert M. Esnouf,[||] Andrew L. Hopkins,[§] Jonathan Warren,[§] Jan Balzarini,[||] David I. Stuart,*[,§,⊥] and David K. Stammers*[,§]

Laboratory of Molecular Biophysics, Rex Richards Building, South Parks Road, Oxford OX1 3QU, U.K., Rega Institute for Medical Research, K. U. Leuven, Minderbroedersstraat 10, B-3000 Leuven, Belgium, and Oxford Centre for Molecular Sciences, New Chemistry Building, South Parks Road, Oxford OX1 3QT, U.K.

Received June 2, 1998; Revised Manuscript Received August 7, 1998

ABSTRACT: The carboxanilides are nonnucleoside inhibitors (NNIs) of HIV-1 reverse transcriptase (RT), of potential clinical importance. The compounds differ in potency and in their retention of potency in the face of drug resistance mutations. Whereas UC-84, the prototype compound, only weakly inhibits many RTs bearing single point resistance mutations, inhibition by UC-781 is little affected. It has been proposed that UC-38 and UC-781 may form quaternary complexes with RT at a site other than the known binding pocket of other NNIs. X-ray crystal structures of four HIV-1 RT−carboxanilide complexes (UC-10, UC-38, UC-84, and UC-781) reported here reveal that all four inhibitors bind in the usual NNI site, forming binary 1:1 complexes with RT in the absence of substrates with the amide/thioamide bond in cis conformations. For all four complexes the anilide rings of the inhibitors overlap aromatic rings of many other NNIs bound to RT. In contrast, the second rings of UC-10, UC-84, and UC-781 do not bind in equivalent positions to those of other "two-ring" NNIs such as α-APA or HEPT derivatives. The binding modes most closely resemble that of the structurally dissimilar NNI, Cl-TIBO, with a common hydrogen bond between each carboxanilide NH− group and the main-chain carbonyl oxygen of Lys101. The binding modes differ slightly between the UC-10/UC-781 and UC-38/UC-84 pairs of compounds, apparently related to the shorter isopropylmethanoyl substituents of the anilide rings of UC-38/UC-84, which draws these rings closer to residues Tyr181 and Tyr188. This in turn explains the differences in the effect of mutated residues on the binding of these compounds.

HIV[1] reverse transcriptase (RT) is a multifunctional enzyme that catalyzes RNA-dependent DNA polymerase, DNA-dependent DNA polymerase, and RNase H activities as well as specifically binding its physiological primer, tRNA Lys3. These functions are all required in the replication of HIV, making RT central to the virus life cycle, thus providing a primary target for anti-HIV drugs widely used in the treatment of AIDS. Currently approved anti-RT drugs fall into two main classes (*1*). The nucleoside analogue inhibitors (e.g., AZT, ddI, ddC, d4T, and 3TC) are incorporated into the primer strand in their metabolically activated triphosphate forms, causing termination of DNA synthesis due to their 3′-deoxy configuration (*2*). The nonnucleoside inhibitors (NNIs) are a chemically diverse set of compounds that are largely specific for HIV-1 RT and generally act as noncompetitive inhibitors with respect to the nucleoside triphosphate substrates (*1*, *3*).

The RT molecule is a heterodimer containing 66 kDa (p66) and 51 kDa (p51) subunits. X-ray crystallographic analyses (*4*−*7*) reveal that the p66 subunit is folded into five domains named fingers, palm, thumb, connection, and RNase H (*4*). The p51 subunit lacks the RNase H domain and has a different relative domain arrangement.

Crystallographic studies have also rationalized the mode of inhibition of RT by NNIs whereby the creation of a NNI-binding pocket some 10−15 Å from the polymerase active site (*4*, *7*, *8*) results in a distortion of the active site aspartyl residues (*6*, *9*). This mechanism is also supported by single turnover kinetic studies (*10*).

[†] The Oxford Centre for Molecular Sciences is supported by the BBSRC, MRC, and EPSRC. The work at Leuven was supported in part by Geconcerteerde Onderzoeksacties (GOA) Project No. 95/5 and the Biomedical Health Programme of the European Commission. R.M.E. is funded by the Onderzoeksfonds van de Katholieke Universiteit Leuven; D.I.S. and D.K.S. are funded by the MRC. The AIDS-directed program of the MRC has provided long-term funding for this project with grants to D.I.S. and D.K.S.

[‡] Coordinates and structure factors for the four HIV-1 RT−carboxanilide complexes have been deposited with the Protein Data Bank for release after 12 months. The accession codes are 1RT5 (UC-10), 1RT6 (UC-38), 1RT7 (UC-84), 1RT4 (UC-781), R1RT5SF (UC-10), R1RT6SF (UC-38), R1RT7SF (UC-84), and R1RT4SF (UC-781).

[§] Laboratory of Molecular Biophysics.

[||] Rega Institute for Medical Research.

[⊥] Oxford Centre for Molecular Sciences.

[1] Abbreviations: HIV, human immunodeficiency virus; RT, reverse transcriptase; NNI, nonnucleoside inhibitor; MKC-442, 6-benzyl-1-(ethoxymethyl)-5-isopropyluracil; α-APA, α-(2,6-dichloro)-α-(2-acetyl-5-methylanilino)acetamide; TIBO, tetrahydroimidazo[4,5,1-*jk*][1,1]-benzodiazepin-2(*1H*)-thione; UC-10, *N*-[4-chloro-3-(*tert*-butyloxime)-phenyl]-2-methyl-3-furancarbothiamide; UC-38, 1-(methylethyl)-2-chloro-5-[[[(1-methylethoxy)thioxo]methyl]amino]benzoate; UC-84, 1-(methylethyl)-2-chloro-5-[[(5,6-dihydro-2-methyl-1,4-oxathiin-3-yl)-carbonyl]amino]benzoate; UC-781, *N*-[4-chloro-3-[[(1,1-dimethylethoxy)-imino]methyl]phenyl]-2-methyl-3-furancarbothiamide.

S0006-2960(98)01309-9 CCC: $15.00
Published on Web 09/25/1998

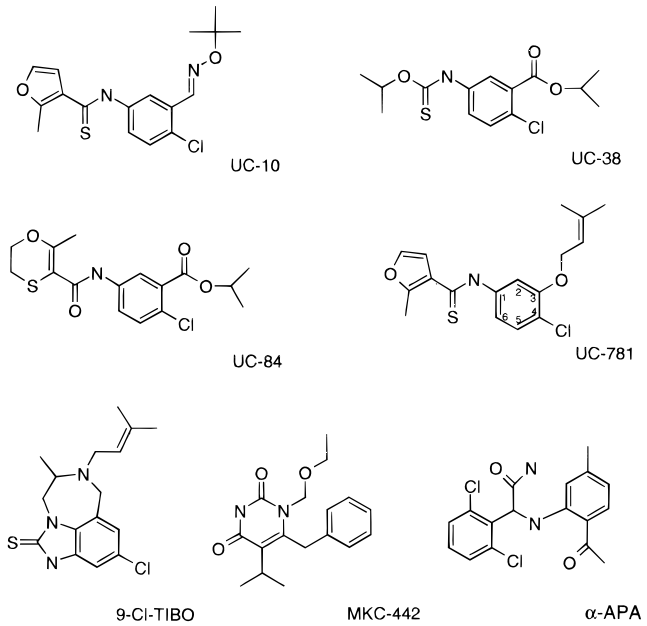

FIGURE 1: Structures of carboxanilide derivatives and three other HIV-1 RT−NNIs, 9-Cl-TIBO, MKC-442, and α-APA.

Table 1: Potency of Carboxanilide Compounds against HIV-1 RT Wild Type and Mutants

HIV-1 strain	EC_{50} (μM) {fold resistance}[a]			
	UC-10	UC-38	UC-84	UC-781
wild type	0.142 {1}	0.029 {1}	0.042 {1}	0.009 {1}
L100I	0.242 {2}	2.06 {71}	>112 {>2700}	0.024 {3}
K103N	1.140 {8}			0.069 {8}
V106A	0.370 {3}	2.06 {71}	>61 {>1500}	0.015 {2}
E138K	0.214 {2}	1.24 {43}	>61 {>1500}	0.015 {2}
V179D	0.480 {4}	0.33 {11}	0.94 {22}	0.017 {2}
Y181C	0.214 {2}	1.9 {66}	42 {1000}	0.033 {4}
Y188H	0.640 {5}	2.1 {72}	2.8 {67}	0.045 {5}

[a] EC_{50} is defined as the concentration of compound required to inhibit syncytia formation in HIV-1-(IIIB)-infected CEM cells (adapted from ref *36*). The fold resistance is the ratio of mutant/wild-type EC_{50}s for each compound.

Although two NNIs (nevirapine and delavirdine) are currently used in anti-HIV combination therapies (*11*, *12*), problems with the selection of drug-resistant mutant HIV RT mean that efforts continue to develop NNIs which are able to inhibit mutant forms of the enzyme. The (thio)-carboxanilide compounds (*13*, *14*), represent one series of "second generation" NNIs, while other examples are the quinoxalines (*15*) and the benzoxazin-2-ones (*16*).

UC-84 (Figure 1) was the first compound in the carboxanilide series to have anti-HIV activity reported, with an EC_{50} of 42 nM (Table 1) (*13*). UC-38 (Figure 1) has similar potency to UC-84 (*17*) but its inhibition is less markedly affected by mutations in RT (Table 1). UC-10 (Figure 1), while being a weaker RT inhibitor than UC-38 (EC_{50} 142 nM), is less affected by single point resistance mutations in RT (*18*, *19*). More recently, UC-781 (Figure 1) has been shown to have a favorable combination of both high potency (EC_{50} 9 nM) together with retention of activity against RTs containing single point mutations such as L100I, K103N, V106A, and Y181C (mutations which give high-level resistance for many NNI series).

Biochemical and kinetic studies of HIV-1 RT inhibition by the carboxanilide series have yielded some surprising results. While UC-84 appeared to be a competitive inhibitor with respect to the template/primer, UC-38 was uncompetitive, implying that the latter compound was not binding to free RT (*20*). By contrast, both compounds appeared to be mixed, noncompetitive inhibitors with respect to the nucleoside triphosphate substrates (*21*). The proposed explanation for such kinetic behavior was the existence of more than one binding site for the inhibitors on RT. Photoprotection experiments with a nevirapine analogue suggested that both UC-38 and UC-84 bound to a site overlapping the nevirapine site, but preferentially bound to different mechanistic forms of the enzyme. UC-38 only gave photoprotection in the presence of template/primer and triphosphate substrates, showing preferential binding within a quaternary complex. Synergistic inhibition of RT enzyme and of HIV in tissue culture has been described for combinations of UC-38 and UC-84 (*20*). UC-781 is reported to be a rapid, tight-binding inhibitor of RT, and photoprotection studies again indicated a preference for binding within a quaternary complex whereas fluorescence-quenching measurements showed direct binding of UC-781 to free RT, albeit in substoichiometric amounts (*22*).

We report here four crystallographic analyses of HIV-1 RT in complexes with different carboxanilides [UC-10, UC-38, UC-84 and UC-781 (Figure 1)], at resolutions between 2.8 and 3.0 Å, aimed at understanding their differing inhibition of mutant RTs as well as providing some clarification of the previous biochemical studies.

MATERIALS AND METHODS

Crystallization and Data Collection. Samples of UC-10, UC-38, UC-84, and UC-781 were provided by Dr. W. Brouwer (Uniroyal Chemical Co., Guelph, ON, Canada). Crystals of complexes of RT with UC-10, UC-38, UC-84, and UC-781 were grown at 4 °C from citrate/phosphate buffer, pH 5.0 (24.25 mM citric acid/51.5 mM Na_2HPO_4), with PEG 3400 (6−10% w/v) as precipitant (*23*). Prior to data collection, crystals were soaked in increasing concentrations of PEG 3400, buffered with the same concentrations of citrate/phosphate buffer used for crystal growth to a maximum PEG 3400 concentration of 50% (w/v). This procedure increases the order of the crystals and results in a series of closely related forms designated A, B, C etc. (*23*, *24*). Inhibitor at a concentration of 0.2 mM was included in the final soak. X-ray diffraction data for complexes of UC-10 and UC-781 with RT were collected on a Weissenberg camera on beamline BL6-A2 (*25*) at the Photon Factory, KEK, Japan, with a 0.1 mm collimator, using the procedures outlined previously (*7*, *26*). Data were collected at 16 °C using 3.5° frames with a coupling constant 1.5°/mm on pairs of 200 × 400 mm Fuji Bas-IIIB imaging plates positioned 429.7 mm from the crystal. The exposure time per frame was between 112 and 140 s depending on the crystal quality. To reduce background noise, the collimator, crystal enclosure, and camera cassette were flooded with helium. The image plates were scanned off-line using Fuji BA 100 IP scanners. Since RT crystals are sensitive to X-ray damage at room temperature, three crystals were used for the RT−

Table 2: Crystallographic Structure Determination Statistics

	RT−UC-10	RT−UC-38	RT−UC-84	RT−UC-781
data collection details				
data collection site, beamline	KEK, BL6-A2	SRS, 7.2	SRS, 9.6	KEK, BL6-A2
temperature (K)	291	100	100	291
wavelength (Å)	1.000	1.488	0.872	1.000
collimation (mm)	0.10	0.20	0.20	0.10
no. of crystals	1	1	1	3
unit cell (Å) (crystal form)[a]	140.3, 111.0, 73.5 (C)	137.0, 109.3, 71.8 (E)	137.6, 109.5, 72.0 (E)	140.4, 111.2, 73.4 (C)
resolution range (Å)	30.0−2.9	30.0−2.8	30.0−3.0	30.0−2.9
observations	67590	84517	53675	101066
unique reflections	22803	26073	19595	24503
completeness (%)	86.1	95.7	87.3	93.6
reflections with $F/\sigma(F) > 3$	17689	21287	15782	20264
R_{merge} (%)[b]	6.2	6.9	10.3	10.1
outer resolution shell				
resolution range (Å)	3.0−2.9	2.9−2.8	3.1−3.0	3.0−2.9
unique reflections	1812	2446	1453	1545
completeness (%)	73.4	91.3	70.8	62.7
reflections with $F/\sigma(F) > 3$	616	1235	794	806
refinement statistics				
resolution range (Å)	30.0−2.9	30.0−2.8	30.0−3.0	30.0−2.9
unique reflections	22763	26069	19595	24458
working/test reflections	21625/1138	24862/1207	18767/828	23235/1223
R factor[c]	0.210	0.234	0.252	0.212
$R_{working}/R_{free}$	0.231/0.291	0.236/0.335	0.258/0.334	0.237/0.295
protein atoms	7752	7830	7821	7741
no. of residues omitted[d]	57	47	49	59
inhibitor atoms	23	20	23	22
water molecules	5	96	6	3
rms bond length deviation (Å)	0.006	0.008	0.009	0.006
rms bond angle deviation (deg)	1.4	1.6	1.5	1.3
mean B factor (Å^2)[e]	55/62/34/25	55/62/29/36	43/53/4/30	58/65/21/29
rms backbone B factor deviation (Å^2)[f]	4.6	5.4	5.8	4.8

[a] See refs *9*, *23*, and *24* for definitions of the different crystal forms. [b] $R_{merge} = \sum|I - \langle I\rangle|/\sum\langle I\rangle$. [c] R factor $= \sum|F_o - F_c|/\sum F_o$. [d] Some residues at the N and C termini of both p66 and p51 subunits, at the junction of the fingers and palm domains, and at the $\alpha6-\beta11$ region in p51 are disordered. These were excluded from the models. [e] Mean B factor for main-chain, side-chain, water, and inhibitor atoms, respectively. [f] rms deviation between B factors for bonded main-chain atoms.

UC-781 data set. RT−UC-10 data were collected from a single crystal exposed at two positions.

Data for the UC-38 and UC-84 complexes were collected at the SRS, Daresbury, U.K., from stations PX7.2 and PX9.6, using MAR Research imaging plates (18 cm and 30 cm diameter), respectively (Table 2). Crystals were frozen in liquid propane prior to data collection and maintained at 100 K using an Oxford Cryosystems Cryostream. Frames of 1.5° oscillations were collected with exposure times of 120 s.

Indexing and integration of data images were carried out with DENZO (*27*), and data were merged with SCALEPACK (*27*). Statistics are given in Table 2.

Structure Solution and Refinement. The structures were all solved by molecular replacement. The model used for the RT−UC-10 and RT−UC-781 complexes was the RT−1051U91 complex [refined at 2.2 Å resolution to an R factor of 0.214; PDB 1RTH (*7*)]. The RT−MKC-442 complex model [refined at 2.55 Å resolution, with an R factor of 0.197; PDB 1RT1 (*28*)] was used for the RT−UC-38 and RT−UC-84 complexes. All water and inhibitor molecules were excluded from the starting models. The molecular orientation and position for each complex were optimized by rigid-body refinement [program X-PLOR (*29*)]. The models were initially treated as single rigid bodies, then as two subunits, and finally as separate rigid groups corresponding to the nine domains of the heterodimer. The data used were gradually extended from 12 to 6.0 Å to the maximum resolution of each data set. At this stage, anisotropic B factor scaling was used to compensate for the anisotropy in the diffraction and to sharpen the data. First, each model was refined using positional and individual atomic B factor refinement against data higher than 7.0 Å resolution. Strong stereochemical restraints were applied to all atoms and positional restraints to those lying greater than 25 Å from the Cα atom of residue 188 (approximately defining the NNI binding pocket). Second, anisotropic B factor scaling for data from 7.0 Å to the maximum resolution was performed against structure factors calculated from models with atomic B factors scaled down by 30%. Third, the coordinates were refined against these scaled data, by positional and B factor refinements. Finally, the original complete data set was scaled with anisotropic B factor scaling against solvent-corrected structure factors calculated from the newly refined models. This procedure [performed with X-PLOR (*29*)] significantly decreased the R factors (as well as the free R factors) for high-resolution shells. The final scaled data sets were used for all subsequent refinements.

The first round of refinement consisted of positional and individual atomic B factor refinements (restrained as above) against all data using a bulk solvent correction. $|F_o| - |F_c|$ maps for all the RT−carboxanilide complexes allowed the inhibitors to be positioned and oriented without difficulty.

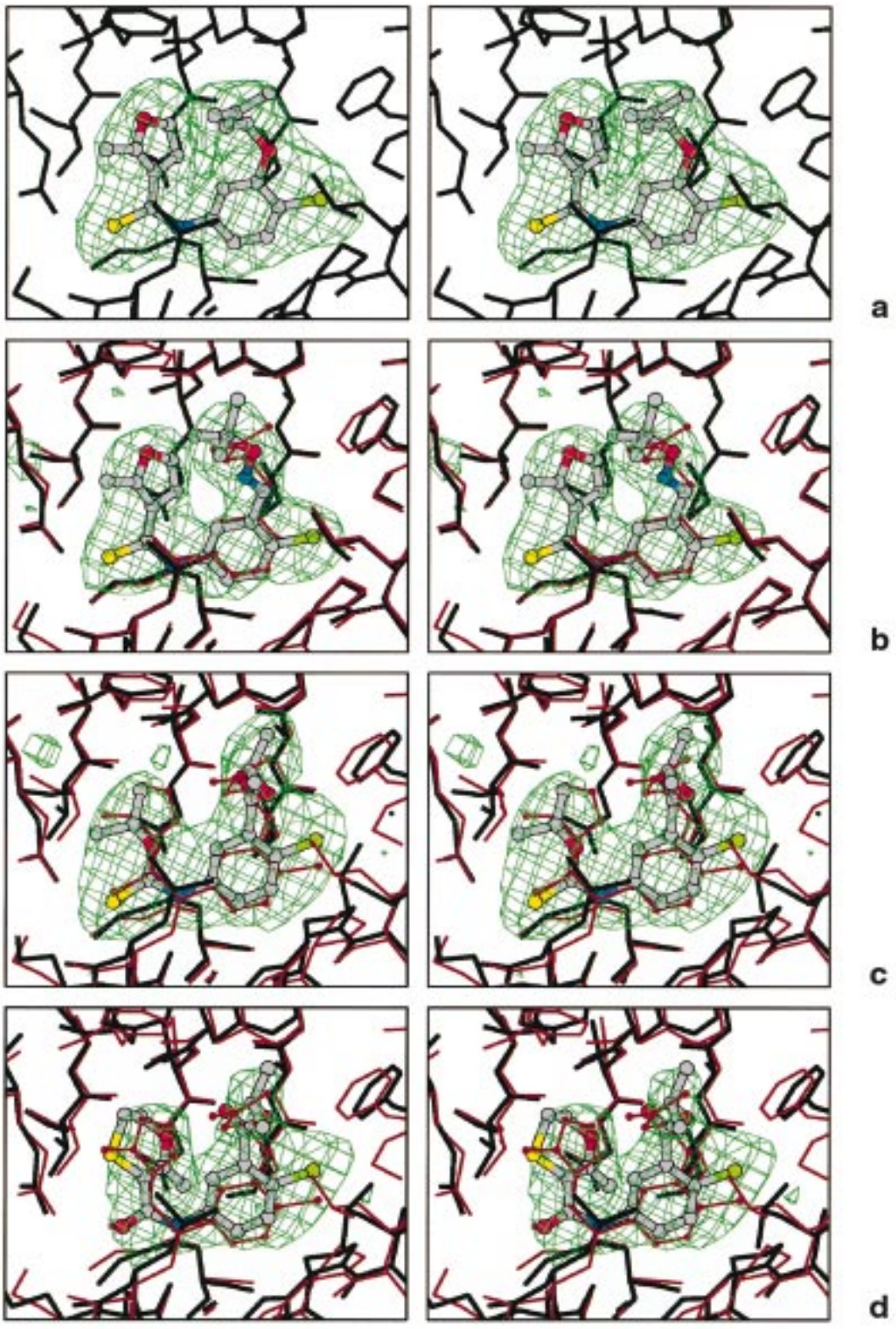

FIGURE 2: Stereoviews of omit $|F_o| - |F_c|$ maps contoured at 3σ showing the electron density for the inhibitors (a) RT−UC-781, (b) RT−UC-10, (c) RT−UC-38, and (d) RT−UC-84. The atoms of the inhibitors are shown in conventional atom colors. The surrounding protein structures are shown in black in each case. The structure of RT−UC-781 is also superimposed in (b), (c), and (d) for comparison, where it is colored brick red. The maps were phased using models from which the inhibitor had been removed followed by further refinement.

Manual model rebuilding used FRODO (*30*) on an Evans and Sutherland ESV workstation. Further rounds of restrained refinement and manual rebuilding resulted in the current models (Table 2; Figure 2). No simulated annealing was performed. Illustrations were prepared using BOBSCRIPT (*31*) and RASTER3D (*32*).

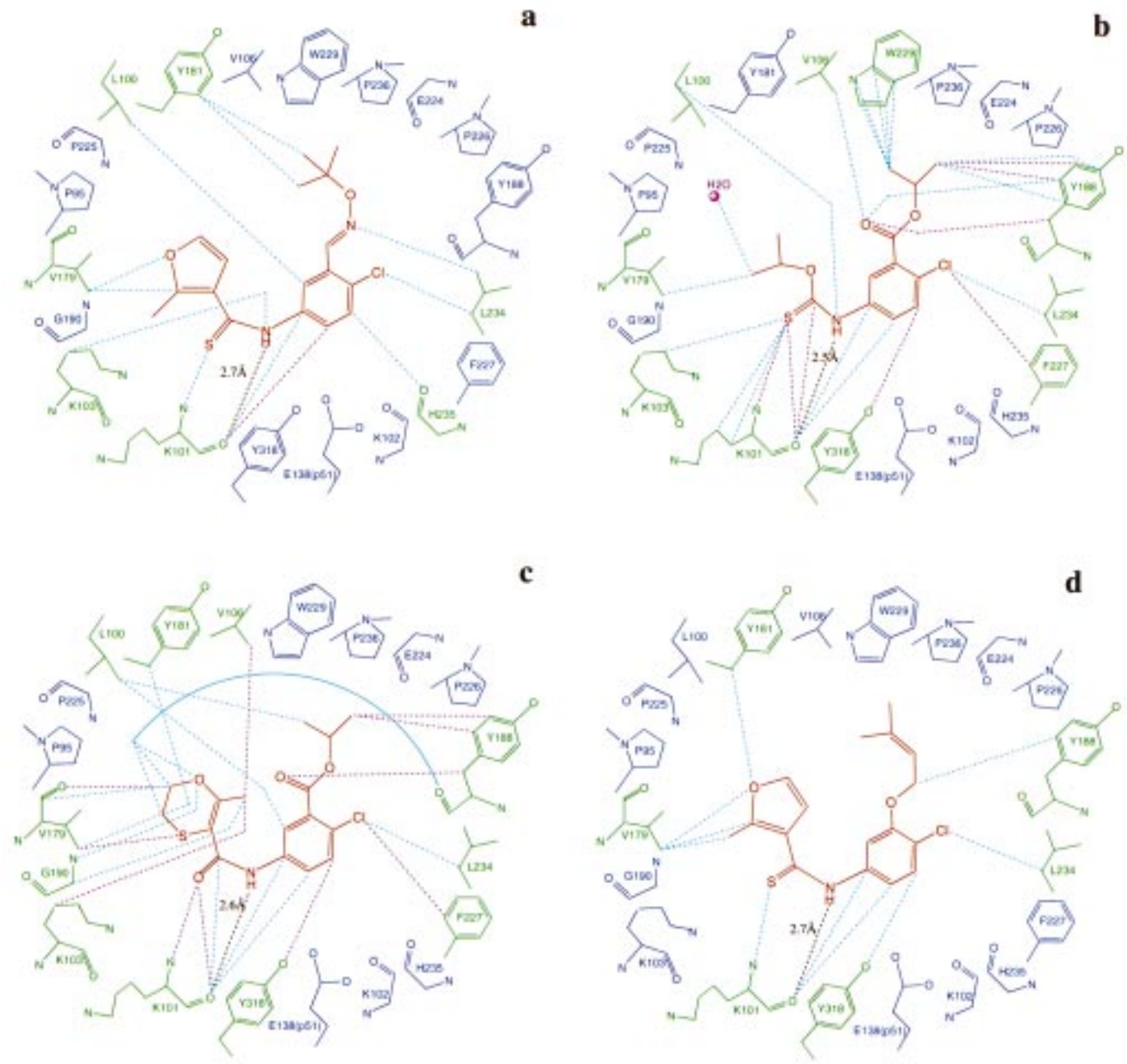

FIGURE 3: Schematic drawings of RT−NNI interactions for (a) UC-10, (b) UC-38, (c) UC-84, and (d) UC-781. All residues that have at least one contact with an NNI within 3.6 Å are shown. A water molecule is shown as a pink sphere in (b). Residues in contact with each NNI are shown in green; otherwise, they are shown in dark blue. Distances between protein and NNI atoms are indicated by broken lines ($d \leq 3.3$ Å in pink; $3.3 < d \leq 3.6$ Å in light blue; H-bonds with distances in black).

RESULTS

General Structural Features. The RT−UC-10 and RT−UC-781 models have been refined to *R* factors of 0.210 and 0.212, respectively, for all data from 30.0 to 2.9 Å resolution. For RT−UC-38 and RT−UC-84 the *R* factors are 0.234 (30.0−2.8 Å resolution) and 0.252 (30.0−3.0 Å resolution), respectively. For all four structures the stereochemistry is excellent (Table 2). Although determined to lower resolution than some of the RT−NNI complexes we have reported previously (*7*, *28*, *33*, *34*), the electron density maps for these complexes after refinement were of good quality, especially around the NNI-binding pockets. The secondary structure nomenclature used here is as described previously (*7*). Some small sections of the protein had no clearly defined electron density in each of the four complexes, and these parts were omitted from the models (Table 2). The conformations of all four inhibitors were well-defined in $|F_o| - |F_c|$ maps.

Figure 3 summarizes the contacts between the inhibitors and RT in each of the four complexes. In each crystal structure strong electron density indicates full occupancy of the inhibitor (Figure 2), and there is no further density consistent with the presence of secondary binding sites. A common feature of the binding of all four inhibitors is the presence of a hydrogen bond (Figures 3 and 4) between the amide or thioamide nitrogen and the main-chain oxygen of Lys101. Equivalent hydrogen bonds have been observed in other RT−NNI complexes (*7*, *28*, *33*). This hydrogen bond forms an anchor around which the carboxanilide inhibitors

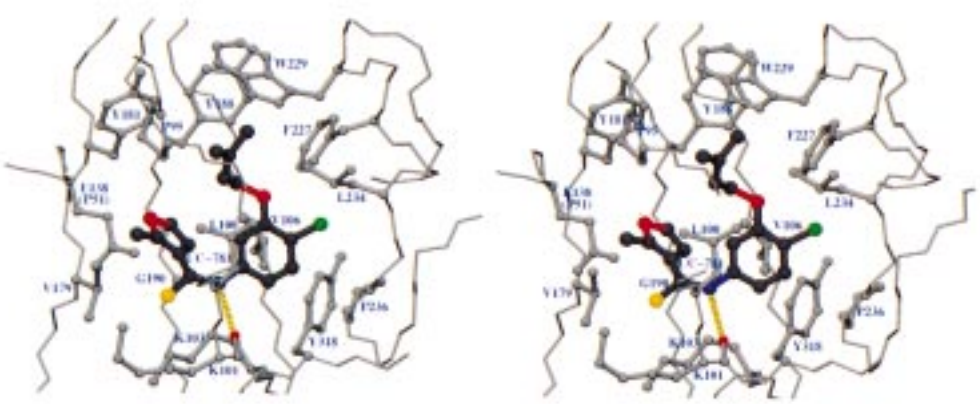

FIGURE 4: Stereo diagram of UC-781 in the NNI pocket. The inhibitor is shown with conventional atom colors, protein side chains are in gray ball-and-stick representation, and the protein backbone is shown as thin sticks. The H-bond from the inhibitor to Lys101 is shown as a dashed yellow line.

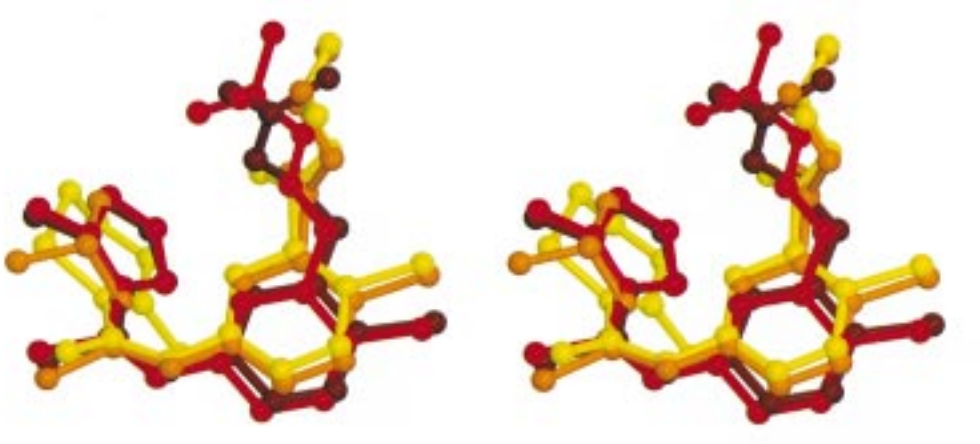

FIGURE 5: Stereo diagram showing the overlap of the RT-bound UC-10 (red), UC-38 (orange), UC-84 (yellow), and UC-781 (brown). The superimposition was carried out using the Cα atoms of amino acid residues around the NNI pocket to compensate for different crystal forms and domain rearrangements. Residues used were 94−118, 156−215, and 225−243 from the palm domain, 317−319 from the connection domain (all from p66), and 137−139 from the fingers domain of p51.

can pivot, and although the phenyl ring defines the overall inhibitor orientation, the differing 3-substituents on this ring can provide a fine-tuning mechanism, which results in the four inhibitors being divided into two groups of two (Figure 5; described in more detail below). One group (UC-38 and UC-84) has the 4-chloro tilted more toward residue Tyr188 than the other group (UC-10 and UC-781).

Position and Conformation of Bound Inhibitors. In the complexes with RT, the carboxanilides are positioned in regions of the NNI-binding pocket commonly occupied by other NNIs (*7*, *28*, *33*), the major exception being in the case of BHAP U-90152 (*34*). The conformation of the protein surrounding the carboxanilides is very similar to that of other RT−NNI complexes, the exceptions being HEPT (*7*, *28*) and BHAP (*34*).

All four carboxanilide inhibitors bind with their (thio)-carboxamide groups in the cis conformation. This, in turn, results in the binding modes of UC-10, UC-84, and UC-781 being different from those of other two-ringed inhibitors such as α-APA and HEPT derivatives (*7*, *28*) (Figure 6). While the carboxanilide rings partially occupy the space of the pyrimidine ring of MKC-442 or the dichlorophenyl ring of α-APA, the furanyl and oxathiinyl rings overlap the space of the isopropyl group of MKC-442 or the amide group of α-APA rather than that of the second rings of MKC-442 (phenyl) or α-APA (methylacetanilide). The volume associated with the second rings of MKC-442 or α-APA is instead partially occupied by the 3-substituents on the carboxanilide rings. In terms of bound conformation, the closest analogue to the carboxanilide compounds is 9-Cl-TIBO (*33*) despite the differences in chemical structure. For UC-781, part of the furanyl ring, the thiocarboxanilide group, and the ether group are analogous to the three fused rings of 9-Cl-TIBO, while the remaining portion of the furanyl ring is aligned with the 5-methyl group and the dimethylallyl group mimics the equivalent moiety in 9-Cl-TIBO (Figure 6). The sulfur and chlorine atoms lie at almost the same positions as those of 9-Cl-TIBO, and there is an equivalent hydrogen bond to the main-chain oxygen of Lys101. The bound conformations of UC-10, UC-38, and UC-84 are similar to that of UC-781, although chemical differences in these inhibitors introduce subtle changes (Figure 3). UC-84 has a 2-methyloxathiin moiety linked to a carboxanilide instead of a 2-methylfuranyl group attached to a thiocarboxanilide as in UC-781. While the small molecule crystal structure of UC-84 shows it to be very flat, with the

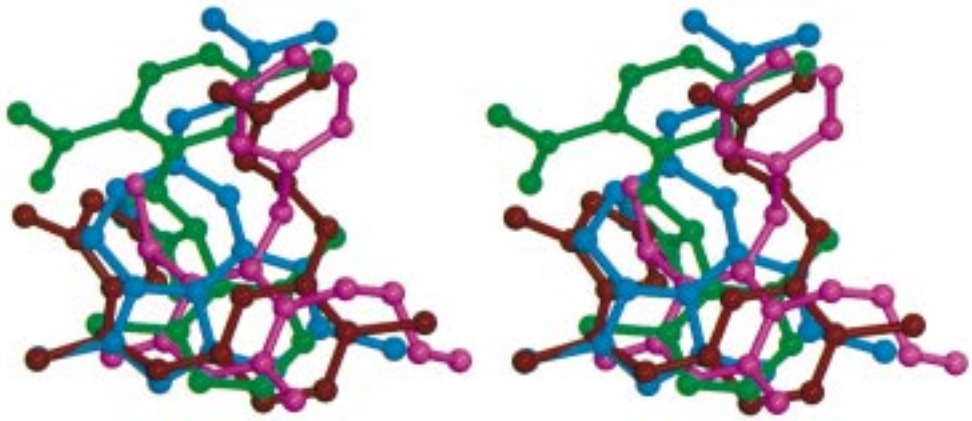

FIGURE 6: Stereo diagram showing the relative positions and orientations of four RT-bound NNIs. UC-781 is shown in brown, α-APA in green, 9-Cl-TIBO in blue, and MKC-442 in magenta. The superimposition was carried out as described for Figure 5.

carboxamide group in a trans conformation (*35*), this group adopts a cis conformation when bound to RT, similar to the other carboxanilide compounds described here. The UC-84 oxathiin 2-methyl group points in the opposite direction to the 2-methyl group of both UC-10 and UC-781, thus exposing its sulfur atom to the solvent. However, due to the limited resolution of the RT−UC-84 structure the pucker of the oxathiin ring is not clearly defined.

Detailed Comparison of Inhibitor−Enzyme Interactions. UC-10 and UC-781 only differ in their 3-substituents, and their common parts bind in an almost identical fashion and make largely equivalent interactions with the protein (Figure 3a,d). In addition to hydrogen bond interactions between the thiocarboxamide nitrogen and the main-chain carbonyl oxygen of Lys101, there are electrostatic interactions between the inhibitor sulfur atoms and the main-chain NH atoms of Lys101. The remaining interactions are via mainly hydrophobic contacts, including those between the furan rings and Val179 and between the chlorophenyl moiety and Leu100, Phe227, Leu234, Pro236, and Tyr318 (Figure 3a,d). In neither case are there significant protein conformational differences compared to the 9-Cl-TIBO complex (*7*).

The differing substituents at the 3-position of the phenyl ring (i.e., *tert*-butyloxime ether for UC-10 and pentenyloxy ether for UC-781) make slightly different hydrophobic interactions with the protein. While common contacts with Tyr181, Tyr188, and Leu234 are observed, the *tert*-butyl group of UC-10 also contacts the side chain of Leu100. The *tert*-butyl group of UC-10 approaches closer than 4.0 Å to the side chain of Trp229, whereas the corresponding dimethylallyl moiety of UC-781 is somewhat further away.

UC-38 and UC-84 have identical 3-isopropylmethanoyl substituents, which, being somewhat smaller than those of UC-10 and UC-781, appear to pull the phenyl rings closer to top of the NNI pocket (i.e., closer to Tyr188). In both cases, this results in small reorientations of Leu100 and Tyr318, as well as a closer approach of the terminal methyl groups of both inhibitors to Leu234, giving a reorientation of this side chain. The remaining interactions for UC-84 with RT involve a close contact of the sulfur of the oxathiin ring with the Val179 side chain; in contrast, UC-38 lacks this interaction as it has a smaller isopropyl ether group.

In all four structures the χ_2 torsion angle of Trp229 differs by about 180° from those observed in other RT−NNI complexes (*7*, *28*, *33*) but is similar to that of the unliganded RT (*9*) (Figure 7). We also observe in all four $|F_o| - |F_c|$ electron density maps an additional strong feature associated with Trp229. This appears to be too strong for a water molecule, and with distances (from the center of the peak) of ∼4.4 Å to Nε1 of Trp229, Nδ1 of His96, and O of Met230, it has been modeled as a phosphate ion.

DISCUSSION

Photoprotection studies have suggested that UC-781 does not bind to the free form of the enzyme, while other experiments indicate direct binding of UC-781 to free RT, but at a stoichiometry of less than 1:1 (*22*). Additionally, kinetic studies have been interpreted to indicate that both UC-38 and UC-781 preferentially bind in ternary complexes with RT and substrates (*21*, *22*). From these data it has been suggested that UC-781 only has significant contacts with Tyr181 in the RT−template/primer−dNTP complex or, alternatively, that it might bind at a site distinct from the NNI site (*22*).

Our results clearly indicate that each of the four carboxanilide compounds binds to the NNI site on RT in the absence of substrates such as template/primer or nucleoside triphosphates. We observe full occupancy of the NNI site and no significant secondary binding sites, thereby giving 1:1 complexes of carboxanilide with the RT heterodimer. We also observe significant contacts between UC-781 and the side chain of Tyr181 in the binary complex with RT. Although it is possible that the binding of these inhibitors might be more complex in the presence of substrates, nevertheless our results fully explain the observed data on the location and effect of escape mutations and cross-resistance studies with other mutant forms of RT (*36*). We thus believe our structural results are consistent with the main biological properties of these compounds.

Analysis of the interactions of the different carboxanilide inhibitors with RT allows us to rationalize the varying inhibitory potency of these compounds. UC-781 has an EC_{50} for RT inhibition approximately 15-fold lower than UC-10 (Table 1), yet the only difference in structure is in the 3-substituents on the carboxanilide ring (Figure 1), and the binding modes are essentially identical. It appears that a number of effects contribute to the greater potency of UC-

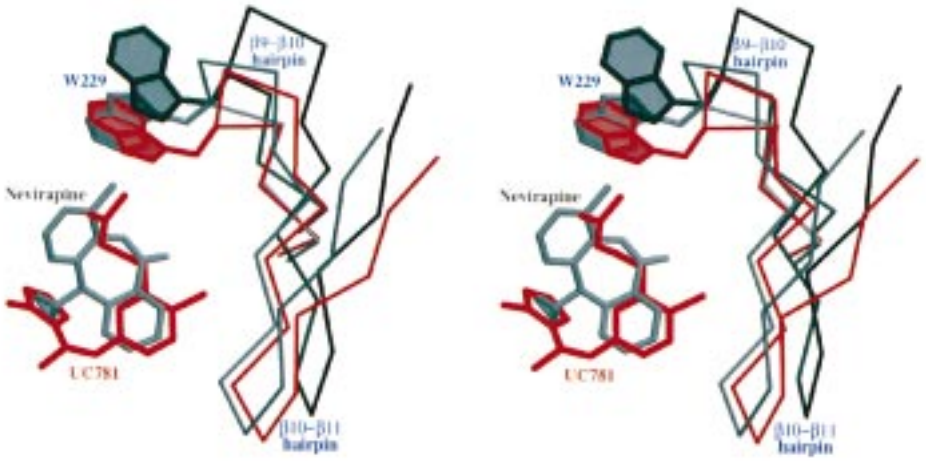

FIGURE 7: Stereo diagram showing the effect of different NNIs on the structure of the β9-β10-β11 sheet and the conformation of Trp229 in different RT−NNI complexes. The β-sheet in RT−nevirapine is shown in gray. The RT−UC-781 complex is shown in red. For comparison, the structure of the β-sheet in unliganded RT is also shown (in black). The superimposition of these structures was carried out as described for Figure 5 except for the omission of amino acids within this β-sheet (residues 225−243). Although only three structures are shown (for clarity), all four RT−carboxanilide complexes are in fact very similar. The RT−nevirapine complex is essentially identical to RT−α-APA and RT−9-Cl-TIBO. Some complexes, for example, RT−MKC-442 and RT−BHAP, have intermediate conformations.

781. First, the UC-781 pentenyloxy group is more hydrophobic than the corresponding oxime ether group of UC-10, thus favoring binding in this most hydrophobic part of the NNI pocket. Additionally, the double bond of the pentenyloxy group of UC-781 is better positioned to make favorable dispersion interactions with the π-clouds of the aromatic side chains of Tyr181 and Tyr188 than is the double bond of the oxime ether group of UC-10.

UC-38 binds with comparable affinity to UC-84 even though the former lacks the oxathiin ring, which for UC-84 makes favorable contacts with the protein. It seems plausible that the loss of contacts with Val179 in UC-38 is offset by the presence of the sulfur of the thioamide group which appears to be favored by the hydophobic environment.

A comparison of the experimentally determined structures of RT−carboxanilides reported here with those based on modeling studies (*36*) shows that, although the predicted binding modes are broadly correct (e.g., the cis conformation and the hydrogen bond to the main chain of Lys101), there are nevertheless some important differences. Esnouf et al. suggested that a stronger interaction of the pentenyl ether group of UC-781 and the side chain of Trp229 than the equivalent interaction involving the *tert*-butyl oxime ether group of UC-10 might explain the difference in affinity for these two compounds. In fact, the UC-10 substituent is more favorably positioned to interact with Trp229, and it appears that other effects explain this difference in binding. Furthermore, the modeling studies did not predict the two pairs of binding modes for UC-10/UC-781 and UC-38/UC-84 nor the rearrangements of Leu234 and Trp229. A key factor in achieving the relatively good prediction was the choice of the RT−9-Cl-TIBO model as the starting point since this protein conformation closely resembles that observed for the RT−carboxanilide complexes described here (with the exception of Trp229).

Yang et al. have modeled UC-40, a close analogue of UC-781, into the RT NNI site (*37*). They report a trans conformation for the thiocarboxamide group in contrast to the cis conformations we observe for UC-781 and the other three carboxanilides. Furthermore, this model has the positions of the phenyl ring and its 3-substituents roughly interchanged when compared to the RT−UC-781 crystal structure, eliminating the hydrogen bond to Lys101. Given the chemical similarity between UC-40 and UC-781, we believe such a different binding mode to be highly unlikely.

In all four RT−carboxanilide complexes the conformation of the Trp229 side chain differs from that normally observed in RT−NNI complexes (Figure 7). It appears that the carboxanilides bind closer to the β9-β10-β11 sheet than most NNIs and possess relatively small substituents on the phenyl ring. These features allow the β9-β10 hairpin to move toward the NNI pocket, and the Trp229 compensates by swapping its conformation. An intermediate case, where Trp229 can adopt either conformation, is observed in the RT−MKC-442 complex (*28*). However, there are some exceptions to this explanation, most notably the RT−BHAP complex (*34*). Although the isopropylamino group of BHAP is much shorter than the substituents at the 3-position of the phenyl ring of the carboxanilide compounds, the side chain of Trp229 is in the classic NNI bound conformation. It seems likely that in this case the indole ring of BHAP wedges the β-sheet away from the pocket. As noted above, the modified conformation of Trp229 creates a further binding pocket on the surface of the enzyme, occupied in all four RT−carboxanilide complexes by an electron-dense moiety tentatively assigned to one of the buffer components, inorganic phosphate (present at a concentration of approximately 50 mM). If one superposes the loop bearing residue 229 [the primer grip (*5*)] as observed in the RT−carboxanilide complexes with that seen in the complex of RT with dsDNA (*5*), then this binding site is only a few Ångströms from the 3′-terminal phosphate group of the primer DNA strand. Our interpretation, if correct, would have various implications. For instance, interactions between the carboxanilide site and the substrate (primer) site might provide some explanation of the observations that carboxanilides can bind preferentially to different mechanistic forms of RT (*21*, *22*).

We find that the structures of the RT−carboxanilide complexes divide into two groups of two, the shorter 3-substituents on the phenyl ring for UC-38 and UC-84 leading to relative rotations of these inhibitors (Figure 5). From our extensive previous experience which showed no effect of temperature of data collection or crystal form on the inhibitor binding mode (*7*, *24*, *33*), we are confident in these results. This division correlates with the observation that, in contrast to UC-38 and UC-84, inhibition of RT by either UC-10 or UC-781 is relatively little affected by many single point mutations within the NNI site (Table 1). One result of this is to increase the number of close contacts with protein side-chain atoms for UC-38 and UC-84, for example, between UC-84 and Leu100, Lys103 and Tyr188, resulting in greater relative increases in EC_{50}s for mutant forms of RT with changes at these codons. In contrast, there appears no similar explanation for the greater effect of the Glu138 → Lys mutation (from the p51 subunit) on UC-84 binding compared to UC-781, since neither compound approaches closer than 4.0 Å to this residue. However, this mutation results in both an increase in bulk and a dramatic change in the electrostatic properties of the side chain. Either effect may have a role in conferring resistance to the different inhibitors.

The hydrogen bond between the amide groups of all four carboxanilides and the main-chain oxygen of Lys101 is not easily disrupted by side-chain mutations. Additionally, the small nonaromatic groups that interact with the top of the NNI pocket in key interactions with Tyr181 and Tyr188 may be able to adapt better to mutations of these aromatic residues than the equivalently positioned phenyl rings of MKC-442 (*28*) or α-APA (*7*). These factors by themselves are not sufficient to confer resilience to mutations in RT (e.g., for UC-38 and UC-84) but could be significant in combination with the optimal 3-substituents of UC-10 or UC-781.

Effective inhibition of both wild-type and mutant RTs is very sensitive to the size and flexibility of the particular carboxanilide inhibitor. The furanyl rings of UC-10 and UC-781 appear to allow the inhibitors to rearrange to accommodate side-chain differences in the mutated NNI pockets. The extra bulk of the UC-84 oxathiinyl ring severely limits this flexibility, while the smaller UC-38 inhibitor is dependent on fewer interactions within the NNI pocket and hence binding can be more radically affected by a single point mutation. The importance of some conformational flexibility for the carboxanilides is shown by comparison with 9-Cl-TIBO. Although 9-Cl-TIBO makes many interactions with RT similar to UC-781, it is more conformationally restricted and therefore less able to bind to RT containing point mutations in the NNI site.

The search for new NNIs is currently driven by the need to find inhibitors which retain their potency in the face of a number of possible resistance mutations. UC-10 and UC-781, along with the quinoxalines (*15*) and the benzoxazin-2-ones (e.g., DMP-266) (*16*), represent second generation NNIs which are more resilient to the presence of some of these mutations. The determination of the structures of complexes between these compounds and mutant RTs will ultimately be of value in the design of improved inhibitors. In the meanwhile the RT−carboxanilide structures presented here provide the clearest insight into the special features that make these second generation RT NNIs potentially of therapeutic importance.

ACKNOWLEDGMENT

We thank the staff of the SRS, Daresbury Laboratory, U.K., and the Photon Factory, KEK, Japan, for their help with data collection; Richard Bryan and Kathryn Measures for computing support; and Stephen Lee for photographic support. We are grateful to the Uniroyal Chemical Co. (Middlebury, CT, and Guelph, ON, Canada) for their continued interest in the work and particularly to Dr. W. Brouwer for providing the carboxanilide samples used in this study.

REFERENCES

1. De Clercq, E. (1994) *Biochem. Pharmacol. 47*, 155−169.
2. Furman, P. A., Fyfe, J. A., St. Clair, M. H., Weinhold, K., Rideout, J. L., Freeman, G. A., Lehrman, S. N., Bolognesi, D. P., Broder, S., Mitsuya, H., and Barry, D. W. (1986) *Proc. Natl. Acad. Sci. U.S.A. 83*, 8333−8337.
3. De Clercq, E. (1996) *Rev. Med. Virol. 6*, 97−117.
4. Kohlstaedt, L. A., Wang, J., Friedman, J. M., Rice, P. A., and Steitz, T. A. (1992) *Science 256*, 1783−1790.
5. Jacobo-Molina, A., Ding, J. P., Nanni, R. G., Clark, A. D., Jr., Lu, X., Tantillo, C., Williams, R. L., Kamer, G., Ferris, A. L., Clark, P., Hizi, A., Hughes, S. H., and Arnold, E. (1993) *Proc. Natl. Acad. Sci. U.S.A. 90*, 6320−6324.
6. Rodgers, D. W., Gamblin, S. J., Harris, B. A., Ray, S., Culp, J. S., Hellmig, B., Woolf, D. J., Debouck, C., and Harrison, S. C. (1995) *Proc. Natl. Acad. Sci. U.S.A. 92*, 1222−1226.
7. Ren, J., Esnouf, R., Garman, E., Somers, D., Ross, C., Kirby, I., Keeling, J., Darby, G., Jones, Y., Stuart, D., and Stammers, D. (1995) *Nat. Struct. Biol. 2*, 293−302.
8. Ding, J., Das, K., Tantillo, C., Zhang, W., Clark, A. D., Jr., Jessen, S., Lu, X., Hsiou, Y., Jacobo-Molina, A., Andries, K., Pauwels, R., Moereels, H., Koymans, L., Janssen, P. A. J., Smith, R. H., Jr., Kroeger Koepke, R., Michejda, C. J., Hughes, S. H., and Arnold, E. (1995) *Structure 3*, 365−379.
9. Esnouf, R., Ren, J., Ross, C., Jones, Y., Stammers, D., and Stuart, D. (1995) *Nat. Struct. Biol. 2*, 303−308.
10. Spence, R. A., Kati, W. M., Anderson, K. S., and Johnson, K. A. (1995) *Science 267*, 988−993.
11. Wong, J. K., Gunthard, H. F., Havlir, D. V., Zhang, Z. Q., Haase, A. T., Ignacio, C. C., Kwok, S., Emini, E., and Richman, D. D. (1997) *Proc. Natl. Acad. Sci. U.S.A. 94*, 12574−12579.
12. Montaner, J. S., Reiss, P., Cooper, D., Vella, S., Harris, M., Conway, B., Wainberg, M. A., Smith, D., Robinson, P., Hall, D., Myers, M., and Lange, J. M. (1998) *J. Am. Med. Assoc. 279*, 930−937.
13. Bader, J. P., McMahon, J. B., Schultz, R. J., Narayanan, V. L., Pierce, J. B., Harrison, W. A., Weislow, O. S., Midelfort, C. F., Stinson, S. F., and Boyd, M. R. (1991) *Proc. Natl. Acad. Sci. U.S.A. 88*, 6740−6744.
14. Balzarini, J., Brouwer, W. G., Dao, D. C., Osika, E. M., and De Clercq, E. (1996) *Antimicrob. Agents Chemother. 40*, 1454−1466.
15. Kleim, J.-P., Bender, R., Billhardt, U.-M., Meichsner, C., Riess, G., Rosner, M., Winkler, I., and Paessens, A. (1993) *Antimicrob. Agents Chemother. 37*, 1659−1664.
16. Young, S. D., Britcher, S. F., Tran, L. O., Payne, L. S., Lumma, W. C., Lyle, T. A., Huff, J. R., Anderson, P. S., Olsen, D. B., Carroll, S. S., Pettibone, D. J., O'Brien, J. A., Ball, R. G., Balani, S. K., Lin, J. H., Chen, I.-W., Schleif, W. A., Sardana, V. V., Long, W. J., Byrnes, V. W., and Emini, E. A. (1995) *Antimicrob. Agents Chemother. 39*, 2602−2605.
17. Balzarini, J., W. G., B., Felauer, E. E., De Clercq, E, and Karlsson, A. (1995) *Antiviral Res. 27*, 219−236.
18. Buckheit, R. W. J., Kinjerski, T. L., Fliakas-Boltz, V., Russell, J. D., Stup, T. L., Pallansch, L. A., Brouwer, W. G., Dao, D.

C., Harrison, W. A., and Schultz, R. J. (1995) *Antimicrob. Agents Chemother. 39*, 2718−2727.
19. Balzarini, J., Pelemans, H., Aquaro, S., Perno, C. F., Witvrouw, M., Schols, D., De Clercq, E., and Karlsson, A. (1996) *Mol. Pharmacol. 50*, 394−401.
20. Fletcher, R. S., Arion, D., Borkow, G., Wainberg, M. A., Dmitrienko, G. I., and Parniak, M. A. (1995) *Biochemistry 34*, 10106−10112.
21. Fletcher, R. S., Syed, K., Mithani, S., Dmitrienko, G. I., and Parniak, M. A. (1995) *Biochemistry 34*, 4346−4353.
22. Barnard, J., Borkow, G., and Parniak, M. A. (1997) *Biochemistry 36*, 7786−7792.
23. Stammers, D. K., Somers, D. O'N., Ross, C. K., Kirby, I., Ray, P. H., Wilson, J. E., Norman, M., Ren, J. S., Esnouf, R. M., Garman, E. F., Jones, E. Y., and Stuart, D. I. (1994) *J. Mol. Biol. 242*, 586−588.
24. Esnouf, R. M., Ren, J., Garman, E., Somers, D., Ross, C., Jones, E. Y., Stammers, D. K., and Stuart, D. I. (1998) *Acta Crystallogr. D54*, 938−953.
25. Sakabe, N. (1991) *Nucl. Instr. Methods Phys. Res. 303*, 448−463.
26. Stuart, D. I., and Jones, E. Y. (1993) *Curr. Opin. Struct. Biol. 3*, 737−740.
27. Otwinowski, Z. (1993) in *Data collection and Processing* (Sawyer, L., Isaacs, N., and Bailey, S., Eds.) pp 56−62, SERC Daresbury Laboratory, Warrington, England.
28. Hopkins, A. L., Ren, J., Esnouf, R. M., Willcox, B. E., Jones, E. Y., Ross, C., Miyasaka, T., Walker, R. T., Tanaka, H., Stammers, D. K., and Stuart, D. I. (1996) *J. Med. Chem. 39*, 1589−1600.
29. Brünger, A. T. (1992) *X-PLOR Manual*, Yale University Press, New Haven, CT.
30. Jones, T. A. (1985) *Methods Enzymol. 115*, 157−171.
31. Esnouf, R. M. (1997) *J. Mol. Graphics 15*, 132−134.
32. Merritt E. A., and Murphy, M. E. P. (1994) *Acta Crystallogr. D50*, 869−873.
33. Ren, J., Esnouf, R., Hopkins, A., Ross, C., Jones, Y., Stammers, D. and Stuart, D. (1995) *Structure 3*, 915−926.
34. Esnouf, R. M., Ren, J., Hopkins, A. L., Ross, C. K., Jones, E. Y., Stammers, D. K., and Stuart, D. I. (1997) *Proc. Natl. Acad. Sci. U.S.A. 94*, 3984−3989.
35. Silverton, J. V., Quinn, F. R., and Haugwitz, R. D. (1991) *Acta Crystallogr. C47*, 1911−1913.
36. Esnouf, R. M., Stuart, D. I., De Clercq, E., Schwartz, E., and Balzarini, J. (1997) *Biochem. Biophys. Res. Commun. 234*, 458−464.
37. Yang, S. S., Pattabiraman, N., Gussio, R., Pallansch, L., Buckheit, R. W. J., and Bader, J. P. (1997) *Leukemia 11*, 89−92.

BI981309M